Quantum Dynamics of H_2 on Cu(111) at 925 K: Recent Developments of the Static Corrugation Model

Bauke Smits

Theoretical Chemistry
Leiden University

SDSS 2023
Oktober 7, 2023

Heterogeneous catalysis is an important facet of modern life.

1. Haber-Bosch process: fertilizer
   - N_2 dissociation the rate-limiting step.
   - Fe catalyst (+ promotors)

   $$N_2 + 3\ H_2 \longrightarrow 2\ NH_3$$
2. Steam reforming: H_2 production
   - CH_4 dissociation the rate-limiting step.
   - Ni catalyst (+ promotors)

   $$CH_4 + H_2O \longrightarrow CO + 3\ H_2$$
3. Proton exchange membrane fuel cell
   - H_2 dissociation the rate-limiting step.
   - Pt catalyst (+ promotors)

   $$2\ H_2 + O_2 \longrightarrow 2\ H_2O$$

Heterogeneous catalysis is an important facet of modern life.

1. Haber-Bosch process: fertilizer
   - N_2 dissociation the rate-limiting step.
   - Fe catalyst (+ promotors)

   $$N_2 + 3\ H_2 \xrightarrow{Fe} 2\ NH_3$$

2. Steam reforming: H_2 production
   - CH_4 dissociation the rate-limiting step.
   - Ni catalyst (+ promotors)

   $$CH_4 + H_2O \xrightarrow{Ni} CO + 3\ H_2$$

3. Proton exchange membrane fuel cell
   - H_2 dissociation the rate-limiting step.
   - Pt catalyst (+ promotors)

   $$2\ H_2 + O_2 \xrightarrow{Pt} 2\ H_2O$$

Heterogeneous catalysis is an important facet of modern life.

1. Haber-Bosch process: fertilizer
   - N_2 dissociation the rate-limiting step.
   - Fe catalyst (+ promotors), **600 K**

   $$N_2 + 3\,H_2 \xrightarrow{Fe} 2\,NH_3$$
2. Steam reforming: H_2 production
   - CH_4 dissociation the rate-limiting step.
   - Ni catalyst (+ promotors), **1000 K**

   $$CH_4 + H_2O \xrightarrow{Ni} CO + 3\,H_2$$
3. Proton exchange membrane fuel cell
   - H_2 dissociation the rate-limiting step.
   - Pt catalyst (+ promotors), **350 K**

   $$2\,H_2 + O_2 \xrightarrow{Pt} 2\,H_2O$$

- Theory often assumes a perfect, '0 K' lattice.

Heterogeneous catalysis is an important facet of modern life.

1. Haber-Bosch process: fertilizer
   - N_2 dissociation the rate-limiting step.
   - Fe catalyst (+ promotors), **600 K**

   $$N_2 + 3\,H_2 \xrightarrow{Fe} 2\,NH_3$$
2. Steam reforming: H_2 production
   - CH_4 dissociation the rate-limiting step.
   - Ni catalyst (+ promotors), **1000 K**

   $$CH_4 + H_2O \xrightarrow{Ni} CO + 3\,H_2$$
3. Proton exchange membrane fuel cell
   - H_2 dissociation the rate-limiting step.
   - Pt catalyst (+ promotors), **350 K**

   $$2\,H_2 + O_2 \xrightarrow{Pt} 2\,H_2O$$

- Theory often assumes a perfect, '0 K' lattice.

First quantum dynamical simulation of H_2 on thermally distorted surface

System of choice: H_2 on Cu(111)

- H_2 (and D_2) dissociation on a Cu(111) surface is a commonly used benchmark system.
  - A lot of experimental and theoretical data.
- Perfect lattice potential reproduces experiment to within chemical accuracy.
  - Potential energy surface (PES) fitted to SRP-DFT using corrugation reducing procedure (CRP).
  - Surface atoms fixed in their perfect crystal lattice positions.
  - Born-Oppenheimer Static Surface (BOSS).
- Static corrugation method (SCM) statically includes surface temperature effects.

Díaz *et al.*, 2009

Wijzenbroek & Somers, 2012

System of choice: H_2 on Cu(111)

- H_2 (and D_2) dissociation on a Cu(111) surface is a commonly used benchmark system.
  - A lot of experimental and theoretical data.
- Perfect lattice potential reproduces experiment to within chemical accuracy.
  - Potential energy surface (PES) fitted to SRP-DFT using corrugation reducing procedure (CRP).
  - Surface atoms fixed in their perfect crystal lattice positions.
  - Born-Oppenheimer Static Surface (BOSS).
- Static corrugation method (SCM) statically includes surface temperature effects.

Díaz *et al.*, 2009

Wijzenbroek & Somers, 2012

System of choice: H_2 on Cu(111)

- H_2 (and D_2) dissociation on a Cu(111) surface is a commonly used benchmark system.
  - A lot of experimental and theoretical data.
- Perfect lattice potential reproduces experiment to within chemical accuracy.
  - Potential energy surface (PES) fitted to SRP-DFT using corrugation reducing procedure (CRP).
  - Surface atoms fixed in their perfect crystal lattice positions.
  - Born-Oppenheimer Static Surface (BOSS).
- Static corrugation method (SCM) statically includes surface temperature effects.

Díaz *et al.*, 2009

Wijzenbroek & Somers, 2012

Static Corrugation Model (SCM)

BOSS

V_{Coup}

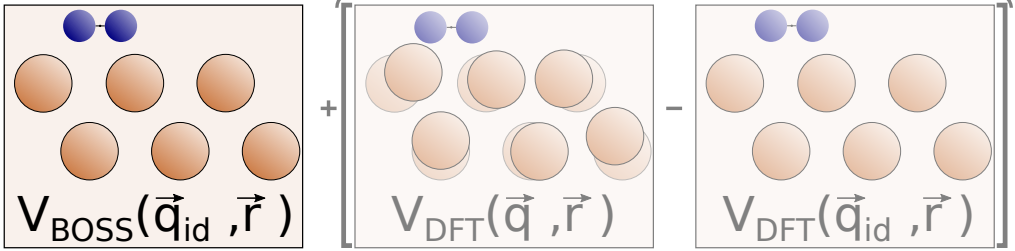

1. $V_{Ideal}(\vec{q}^{\,id}, \vec{r}^{\,id}(\vec{r}))$
2. $+\sum_i^{\vec{r}} \sum_j^{\vec{q}} \left[V_{H\text{-}Cu}(|\vec{r}_i - \vec{q}_j|) - V_{H\text{-}Cu}(|\vec{r}^{\,id}(\vec{r}) - \vec{q}_j^{\,id}|) \right]$

Static Corrugation Model (SCM)

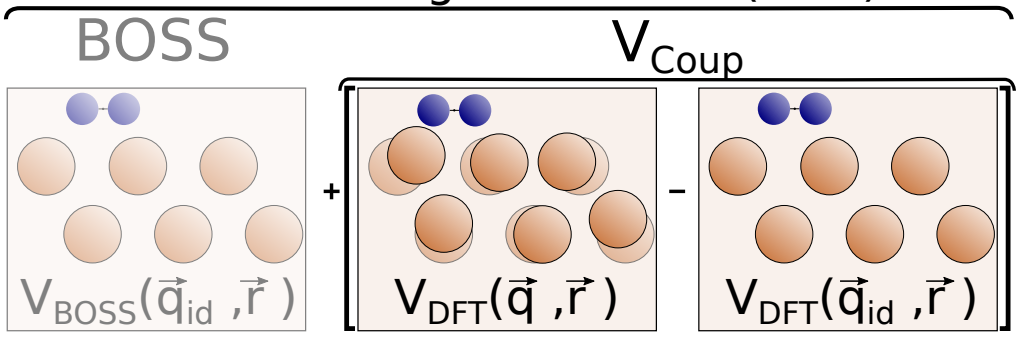

1. $V_{Ideal}(\vec{q}^{\,id}, \vec{r}^{\,id}(\vec{r}))$
2. $+\sum_i^{\vec{r}} \sum_j^{\vec{q}} \left[V_{H\text{-}Cu}(|\vec{r_i} - \vec{q_j}|) - V_{H\text{-}Cu}(|\vec{r}^{\,id}(\vec{r}) - \vec{q_j}^{\,id}|) \right]$

Quantum Dynamics

Time-dependent wave packet (TDWP) approach

1. Propagate H_2 described by WP on 6D PES.
2. Some of the WP scatters back (in different states).
3. Analyse scattered WP and find the probabilities for each state.
4. $P_{reac} = (1 - P_{scattered})$

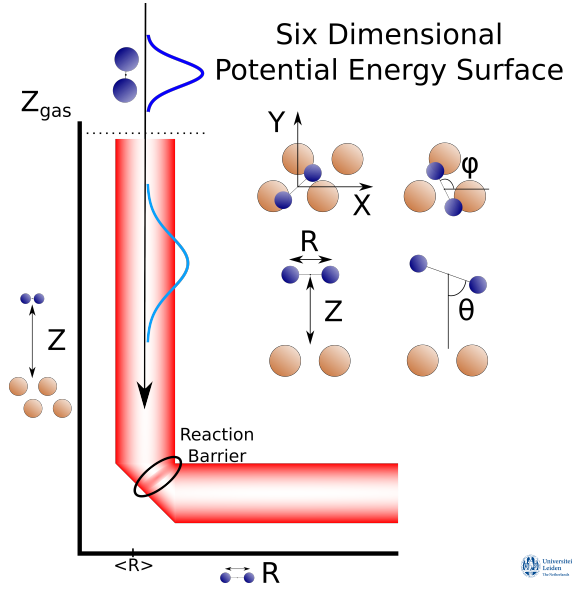

Quantum Dynamics

Time-dependent wave packet (TDWP) approach

1. Propagate H_2 described by WP on 6D PES.
2. Some of the WP scatters back (in different states).
3. Analyse scattered WP and find the probabilities for each state.
4. P_{reac} = (1 - $P_{scattered}$)

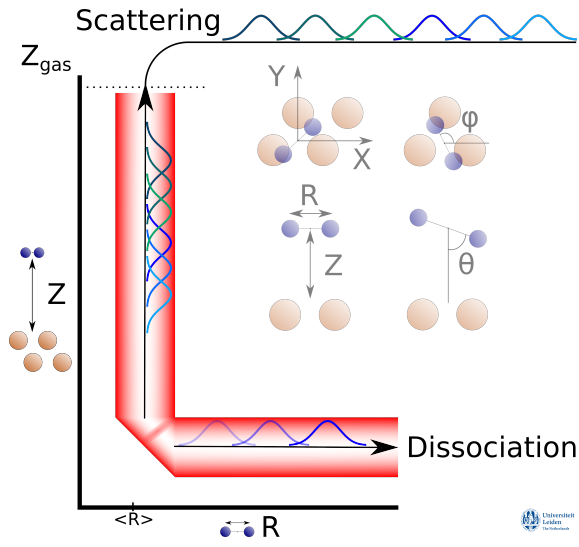

Quantum Dynamics

Time-dependent wave packet (TDWP) approach

1. Propagate H_2 described by WP on 6D PES.
2. Some of the WP scatters back (in different states).
3. Analyse scattered WP and find the probabilities for each state.
4. P_{reac} = (1 - $P_{scattered}$)

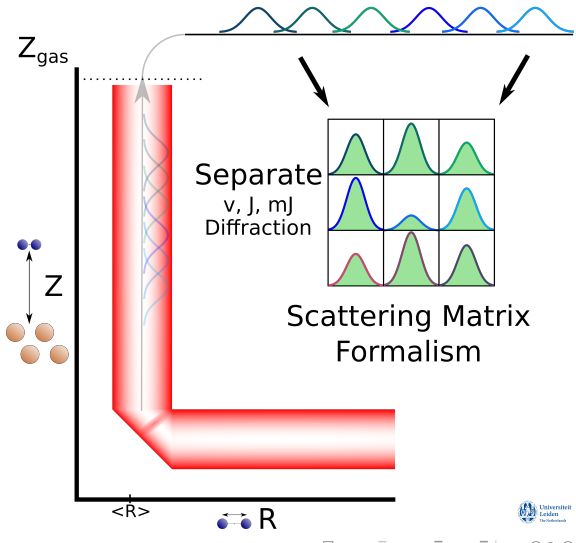

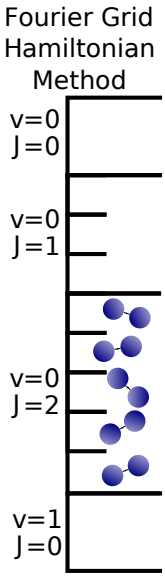

Quasi-classical trajectories

1. Start with a quantized rovibrational state.
2. Molecules freely vibrate and rotate during **classical** dynamics.
3. Scattered molecules are binned to the closest (in rot. energy) **allowed** rotational state.
4. Molecules are binned to the closest (in total energy) rovibrational state with the same rot. state.

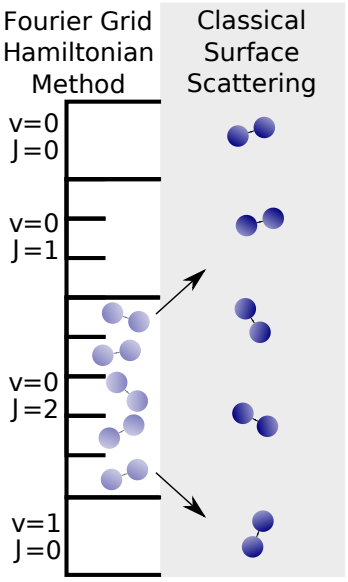

Quasi-classical trajectories

1. Start with a quantized rovibrational state.
2. Molecules freely vibrate and rotate during **classical** dynamics.
3. Scattered molecules are binned to the closest (in rot. energy) **allowed** rotational state.
4. Molecules are binned to the closest (in total energy) rovibrational state with the same rot. state.

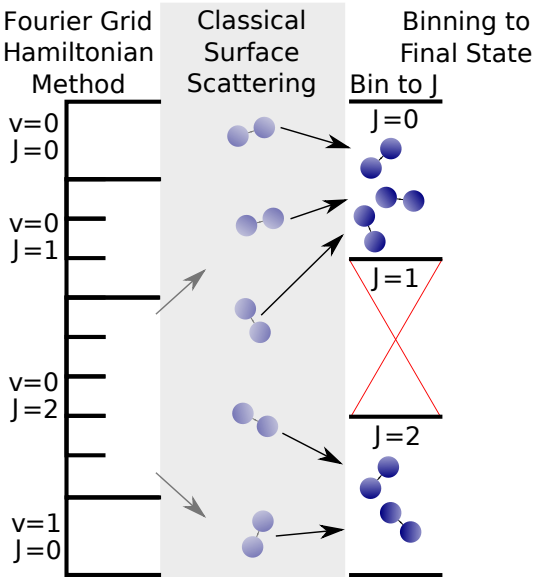

Quasi-classical trajectories

1. Start with a quantized rovibrational state.
2. Molecules freely vibrate and rotate during **classical** dynamics.
3. Scattered molecules are binned to the closest (in rot. energy) **allowed** rotational state.
4. Molecules are binned to the closest (in total energy) rovibrational state with the same rot. state.

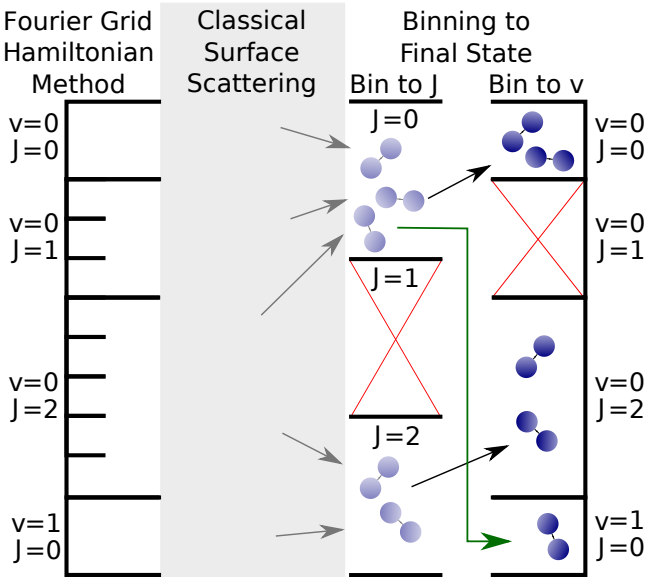

Quasi-classical trajectories

1. Start with a quantized rovibrational state.
2. Molecules freely vibrate and rotate during **classical** dynamics.
3. Scattered molecules are binned to the closest (in rot. energy) **allowed** rotational state.
4. Molecules are binned to the closest (in total energy) rovibrational state with the same rot. state.

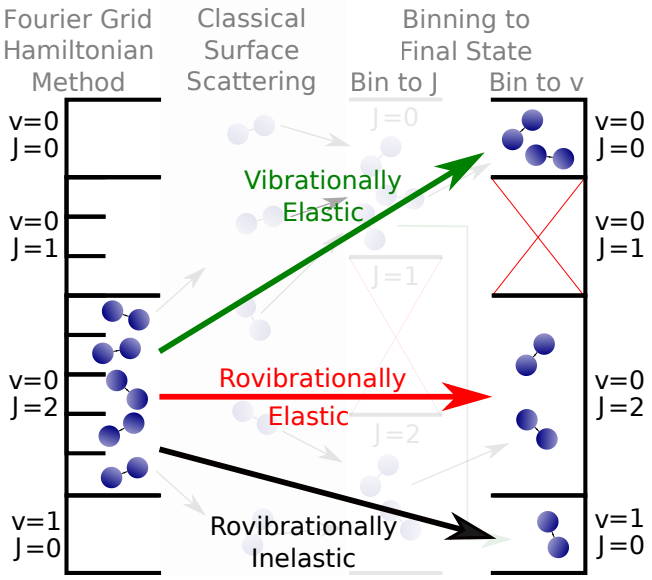

Quasi-classical trajectories

1. Start with a quantized rovibrational state.
2. Molecules freely vibrate and rotate during **classical** dynamics.
3. Scattered molecules are binned to the closest (in rot. energy) **allowed** rotational state.
4. Molecules are binned to the closest (in total energy) rovibrational state with the same rot. state.

Methods - A Summary

- **Born-Oppenheimer Static Surface (BOSS)**
  - PES from SRP48 DFT functional.
  - Surface static in its ideal configuration.
- **Static Corrugation Model (SCM)**
  - Expand BOSS PES with SCM coupling potential.
  - Surface static, but distorted at 925 K.

- **Quantum Dynamics (QD)**
  - Time-dependent wave packet approach.
  - WPs split into several energy ranges.
  - Monte-Carlo sampled distorted surface using 104 configurations.
- **Quasi-Classical Dynamics (QCD)**
  - Classical dynamics with initial quantised states.
  - 50.000 trajectories per incidence energy.
  - Distorted surface randomly chosen every trajectory.

Methods - A Summary

- **Born-Oppenheimer Static Surface (BOSS)**
  - PES from SRP48 DFT functional.
  - Surface static in its ideal configuration.
- **Static Corrugation Model (SCM)**
  - Expand BOSS PES with SCM coupling potential.
  - Surface static, but distorted at 925 K.

- **Quantum Dynamics (QD)**
  - Time-dependent wave packet approach.
  - WPs split into several energy ranges.
  - Monte-Carlo sampled distorted surface using 104 configurations.
- **Quasi-Classical Dynamics (QCD)**
  - Classical dynamics with initial quantised states.
  - 50.000 trajectories per incidence energy.
  - Distorted surface randomly chosen every trajectory.

Methods - A Summary

- **Born-Oppenheimer Static Surface (BOSS)**
  - PES from SRP48 DFT functional.
  - Surface static in its ideal configuration.
- **Static Corrugation Model (SCM)**
  - Expand BOSS PES with SCM coupling potential.
  - Surface static, but distorted at 925 K.

- **Quantum Dynamics (QD)**
  - Time-dependent wave packet approach
  - WPs split into several energy ranges.
  - Monte-Carlo sampled distorted surface using 104 configurations.
- **Quasi-Classical Dynamics (QCD)**
  - Classical dynamics with initial quantised states.
  - 50.000 trajectories per incidence energy.
  - Distorted surface randomly chosen every trajectory.

Methods - A Summary

- **Born-Oppenheimer Static Surface (BOSS)**
  - PES from SRP48 DFT functional.
  - Surface static in its ideal configuration.
- **Static Corrugation Model (SCM)**
  - Expand BOSS PES with SCM coupling potential.
  - Surface static, but distorted at 925 K.

- **Quantum Dynamics (QD)**
  - Time-dependent wave packet approach
  - WPs split into several energy ranges.
  - Monte-Carlo sampled distorted surface using 104 configurations.
- **Quasi-Classical Dynamics (QCD)**
  - Classical dynamics with initial quantised states.
  - 50.000 trajectories per incidence energy.
  - Distorted surface randomly chosen every trajectory.

Magnitude of error due to surface sampling

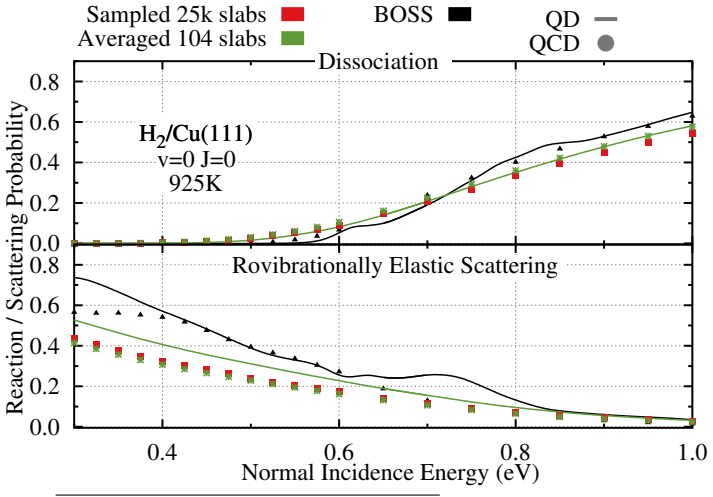

Smits & Somers, 2022

- QCD results averaged over 104 surfaces or random from dataset.
  - Quantifies error limited number of surfaces.
- Minor differences between sampling (QCD) and averaging (QD) of surfaces.
- SCM shows curve broadening.
- Good agreement between QD and QCD of BOSS and SCM.

Magnitude of error due to surface sampling

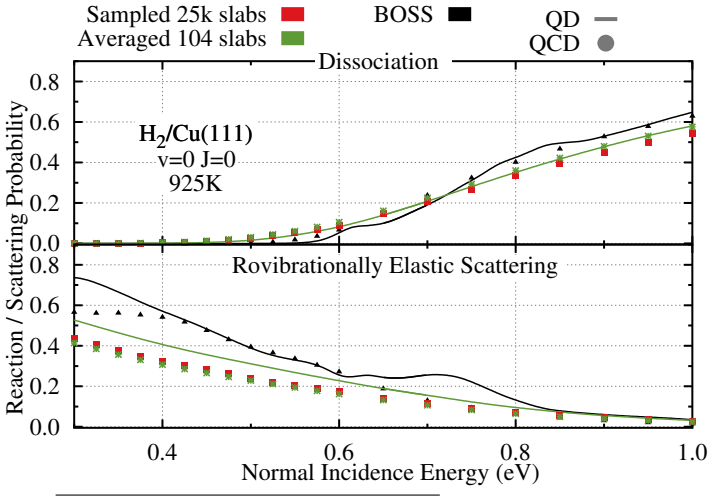

Smits & Somers, 2022

- QCD results averaged over 104 surfaces or random from dataset.
  - Quantifies error limited number of surfaces.
- Minor differences between sampling (QCD) and averaging (QD) of surfaces.
- SCM shows curve broadening.
- Good agreement between QD and QCD of BOSS and SCM.

Single Surface Comparisons

- Results for single surface slabs.
  - Very reactive and non-reactive slabs.
- Reaction probability agreement between QD and QCD is excellent.
- Difference in scattering primarily for non-reactive slab.

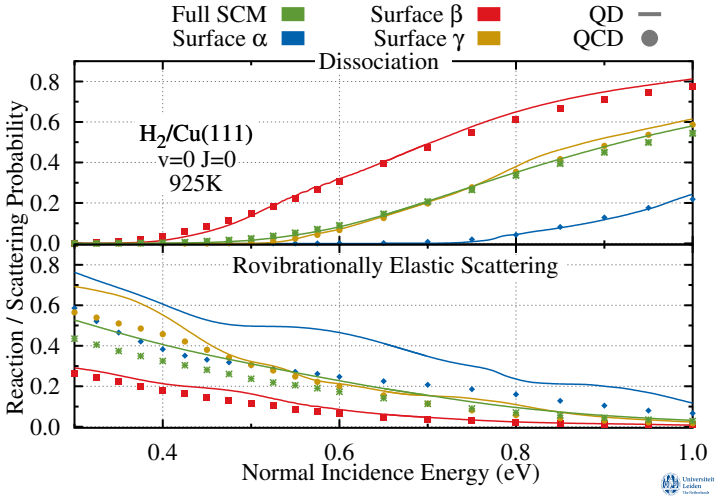

Smits & Somers, 2022

Single Surface Comparisons

- Results for single surface slabs.
  - Very reactive and non-reactive slabs.
- Reaction probability agreement between QD and QCD is excellent.
- Difference in scattering primarily for non-reactive slab.

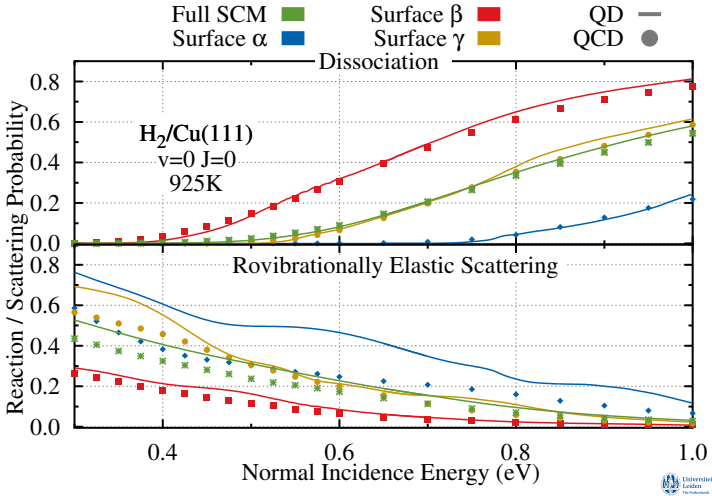

Smits & Somers, 2022

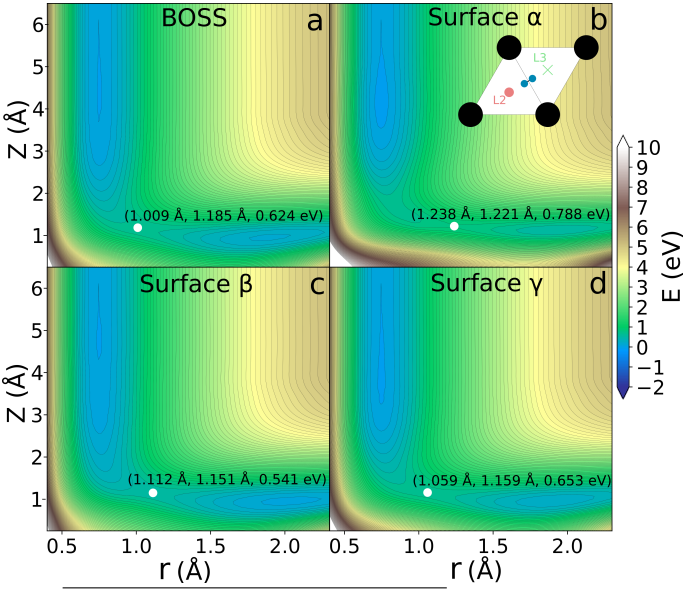

Smits & Somers, 2023

- Bridge-to-hollow site
  - Lowest reaction barrier.
- SCM barriers later in r.
- Little change in Z.
- Geometry around barrier varies.
  - Effect on rot. and vib. efficacies.

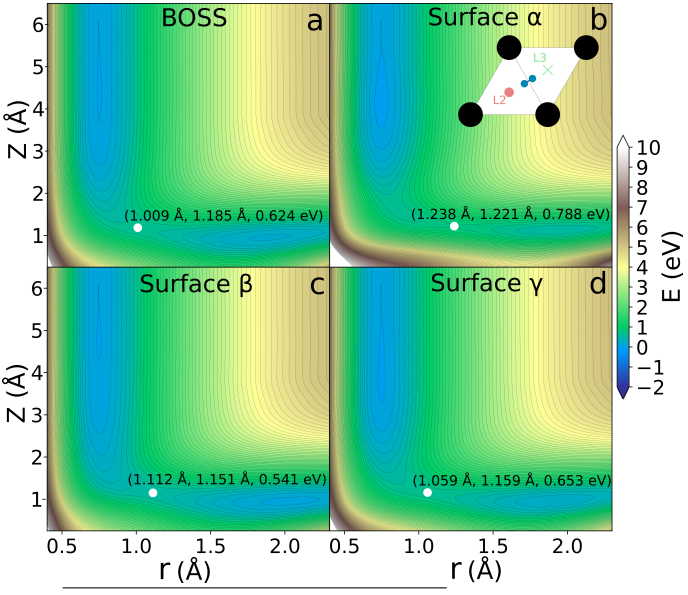

Smits & Somers, 2023

- Bridge-to-hollow site
  - Lowest reaction barrier.
- SCM barriers later in r.
- Little change in Z.
- Geometry around barrier varies.
  - Effect on rot. and vib. efficacies.

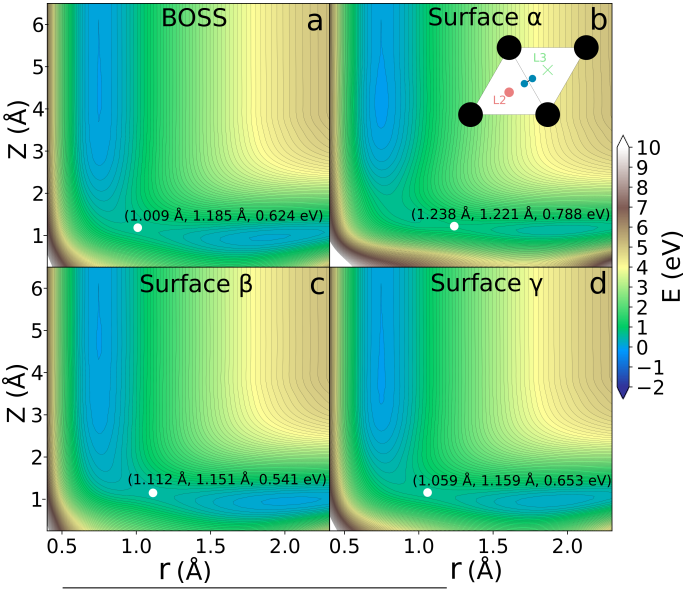

Smits & Somers, 2023

- Bridge-to-hollow site
  - Lowest reaction barrier.
- SCM barriers later in r.
- Little change in Z.
- Geometry around barrier varies.
  - Effect on rot. and vib. efficacies.

- Top-to-fcc site
  - One of the higher barriers.
- Variation in barrier location and height.
- Energetically higher barriers later in r and Z.

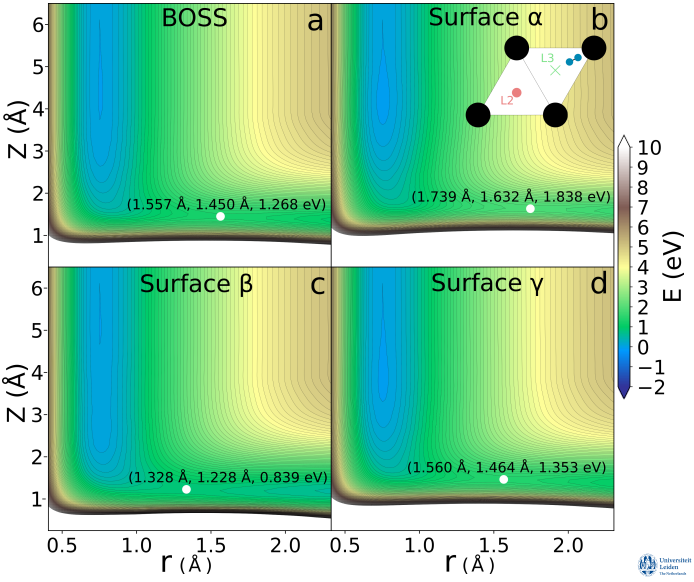

Smits & Somers, 2023

- Top-to-fcc site
  - One of the higher barriers.
- Variation in barrier location and height.
- Energetically higher barriers later in r and Z.

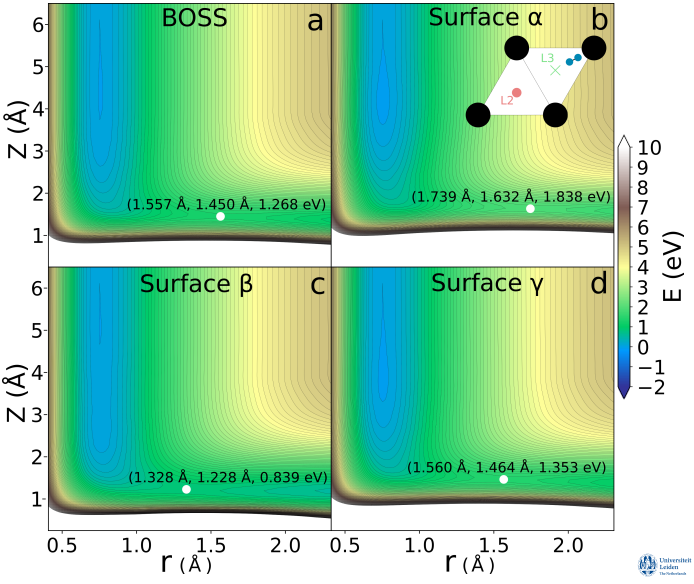

Smits & Somers, 2023

Comparisons to experiment

Compare to experimental results by Kaufmann *et al.* JCP, **148**, 194703 (2018):
Associative desorption of hydrogen isotopologues from copper surfaces: Characterization of two reaction mechanisms

- Desorption experiments of H_2/D_2/HD from Cu(111)/Cu(211).
  - Obtain state-selective time-of-flight spectra.
  - Direct inversion under detailed balance.
- Fit to ERF form + slow channel.
  - Exact W and E_0
  - Only relative saturation values.

$$P_{stick} = \frac{A}{2}\left[1 + \mathrm{erf}\left(\frac{E_{kin} - E_0}{W}\right)\right] + P_{stick}^{slow}$$

A Saturation value
E_0 Energy at half saturation
W Width parameter

Comparisons to experiment

Compare to experimental results by Kaufmann *et al.* JCP, **148**, 194703 (2018):
Associative desorption of hydrogen isotopologues from copper surfaces: Characterization of two reaction mechanisms

- Desorption experiments of H_2/D_2/HD from Cu(111)/Cu(211).
  - Obtain state-selective time-of-flight spectra.
  - Direct inversion under detailed balance.
- Fit to ERF form + slow channel.
  - Exact W and E_0
  - Only relative saturation values.

$$P_{stick} = \frac{A}{2}\left[1 + \mathrm{erf}\left(\frac{E_{kin} - E_0}{W}\right)\right] + P_{stick}^{slow}$$

A Saturation value
E_0 Energy at half saturation
W Width parameter

Comparisons to experiment

Estimate saturation value with other data:

A^{Min}	Beam adsorption experiments
A^{Est}	Theory results at max. energy
A^{Max}	Highest estimate encountered

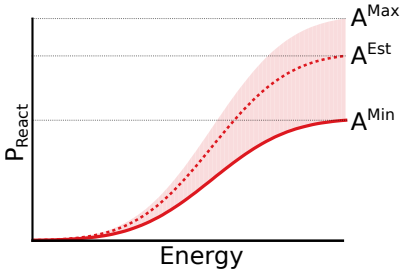

- Fit to ERF form + slow channel.
  - Exact W and E_0
  - Only relative saturation values.

$$P_{stick} = \frac{A}{2}\left[1 + \mathrm{erf}\left(\frac{E_{kin} - E_0}{W}\right)\right] + P_{stick}^{slow}$$

A Saturation value

E_0 Energy at half saturation

W Width parameter

Dissociative Chemisorption

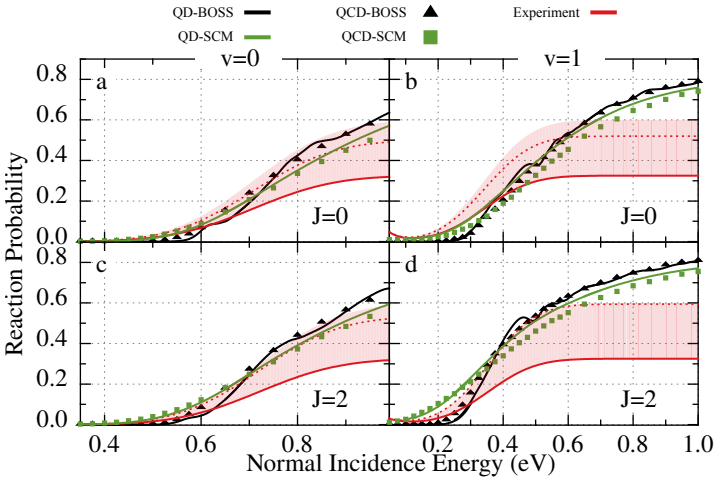

- Some difference QD↔QCD for vib. excited states.
- Agreement with experiment mixed.
  - Good with estimated saturation for v=0.
  - Overestimate for v=1, J=2.
  - For v=1, J=0, good with low saturation.

Kaufmann *et al.*, 2018
Smits & Somers, 2022

Dissociative Chemisorption

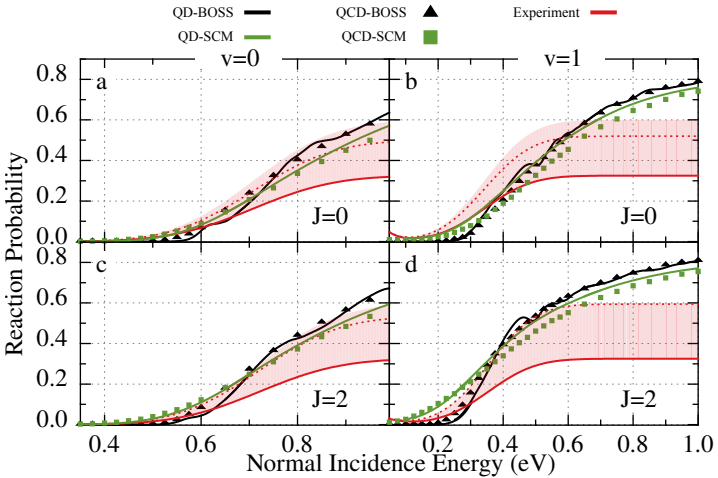

- Some difference QD↔QCD for vib. excited states.
- Agreement with experiment mixed.
  - Good with estimated saturation for v=0.
  - Overestimate for v=1, J=2.
  - For v=1, J=0, good with low saturation.

Kaufmann *et al.*, 2018
Smits & Somers, 2022

Reaction - Logarithmic scale

- With logarithmic reaction scale, we can focus on curve onset.
- Broader curve onset of SCM matches experiment.
- QD results have unphysical shape at low reaction probability.
  - Noise due to timestep.

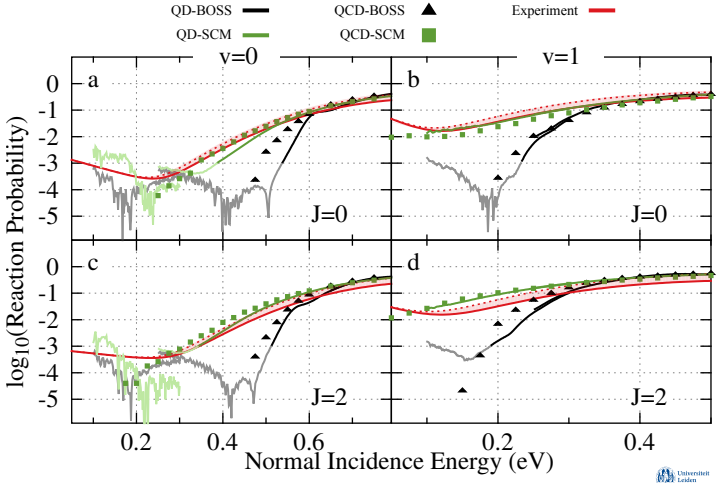

Kaufmann *et al.*, 2018

Smits & Somers, 2022

Reaction - Logarithmic scale

- With logarithmic reaction scale, we can focus on curve onset.
- Broader curve onset of SCM matches experiment.
- QD results have unphysical shape at low reaction probability.
  - Noise due to timestep.

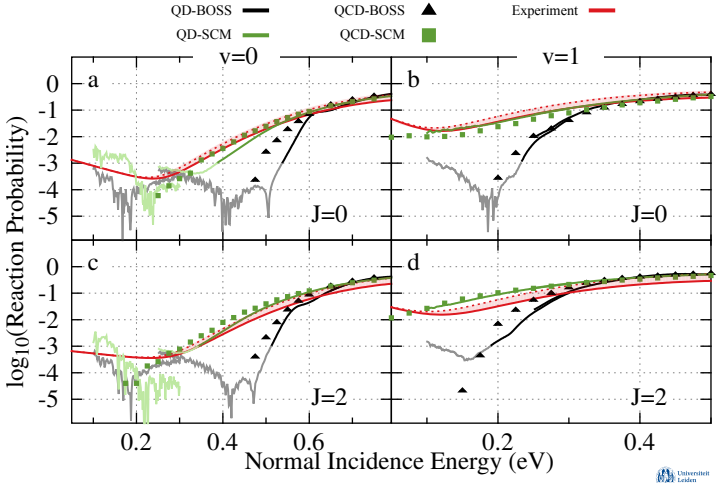

Kaufmann *et al.*, 2018

Smits & Somers, 2022

QD - reducing time step

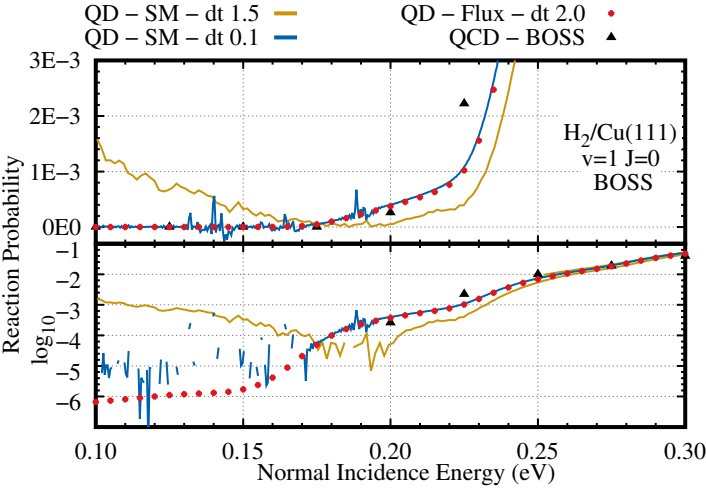

- Much smaller timestep.
- Much longer propagation
- Much larger grids.
- No upturn.
- Slightly affects higher energy of WP.
- Improves agreement with QCD.
- **18 days on 32 cores.**

Smits & Somers, 2023

QD - reducing time step

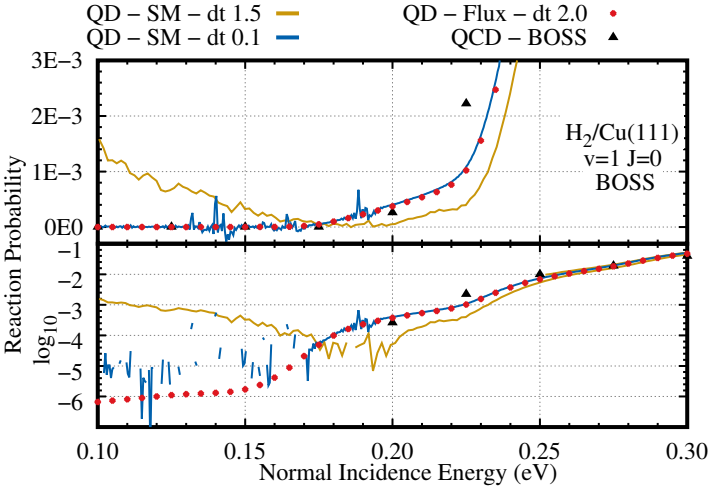

- Much smaller timestep.
- Much longer propagation
- Much larger grids.
- No upturn.
- Slightly affects higher energy of WP.
- Improves agreement with QCD.
- **18 days on 32 cores.**

Smits & Somers, 2023

QD - reducing time step

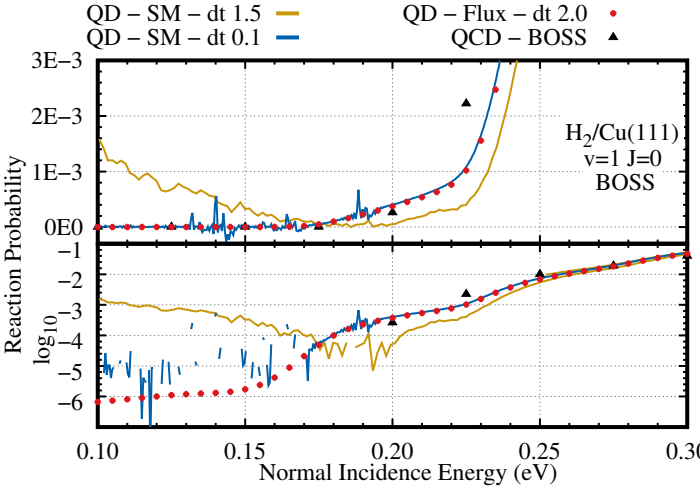

- Much smaller timestep.
- Much longer propagation
- Much larger grids.
- No upturn.
- Slightly affects higher energy of WP.
- Improves agreement with QCD.
- **18 days on 32 cores.**

Smits & Somers, 2023

Time-of-Flight spectra

- Simulated time-of-flight spectra are a more direct comparison to experiment.
  - Remove uncertainty in experimental saturation value.
  - Introduce some errors due fitting P_{stick}.

$$I(t) = K \cdot \exp\left(\frac{-E_n}{2k_b T_s}\right) \cdot \left(\frac{x}{t}\right)^4 \cdot P_{stick}(E_n)$$

with

Gompertz function

$$P_{stick}(E_n) = A \cdot \exp\left[-\exp\left(-\frac{E_n - B}{C}\right)\right]$$

Five-parameter curve

$$P_{stick}(E_n) = \frac{A \cdot \exp\left[-\exp\left(-\frac{E_n - B}{C}\right)\right]}{1 + \exp\left(-\frac{E_n - B_1}{C_1}\right)}$$

Error function

$$P_{stick}(E_n) = \frac{A}{2}\left[1 + \mathrm{erf}\left(\frac{E_n - E_0}{W}\right)\right]$$

Nattino *et al.*, 2014

Time-of-Flight spectra

- Simulated time-of-flight spectra are a more direct comparison to experiment.
  - Remove uncertainty in experimental saturation value.
  - Introduce some errors due fitting P_{stick}.

$$I(t) = K \cdot \exp\left(\frac{-E_n}{2k_b T_s}\right) \cdot \left(\frac{x}{t}\right)^4 \cdot P_{stick}(E_n)$$

with

Gompertz function

$$P_{stick}(E_n) = A \cdot \exp\left[-\exp\left(-\frac{E_n - B}{C}\right)\right]$$

Five-parameter curve

$$P_{stick}(E_n) = \frac{A \cdot \exp\left[-\exp\left(-\frac{E_n - B}{C}\right)\right]}{1 + \exp\left(-\frac{E_n - B_1}{C_1}\right)}$$

Error function

$$P_{stick}(E_n) = \frac{A}{2}\left[1 + \mathrm{erf}\left(\frac{E_n - E_0}{W}\right)\right]$$

Nattino *et al.*, 2014

Time-of-Flight spectra

- SCM broadens spectra.
  - Same as dissociation curves.
- Agreement between QD and QCD better for SCM than BOSS.
- SCM closer to experiment than BOSS (except v=1, J=2).

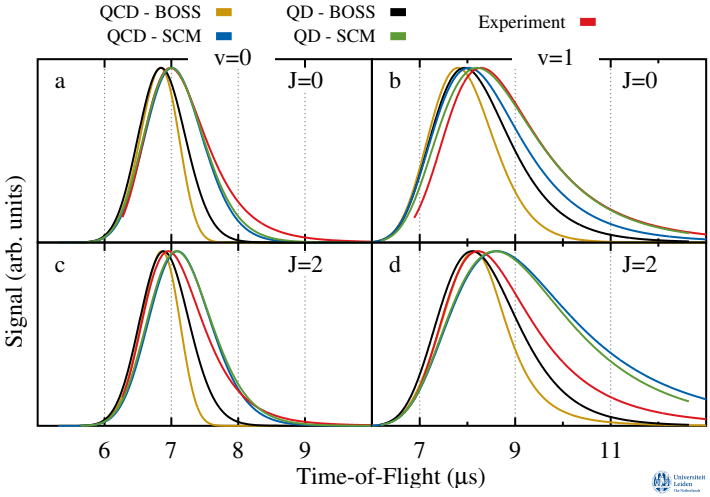

Kaufmann *et al.*, 2018
Smits & Somers, 2023

Time-of-Flight spectra

- SCM broadens spectra.
  - Same as dissociation curves.
- Agreement between QD and QCD better for SCM than BOSS.
- SCM closer to experiment than BOSS (except v=1, J=2).

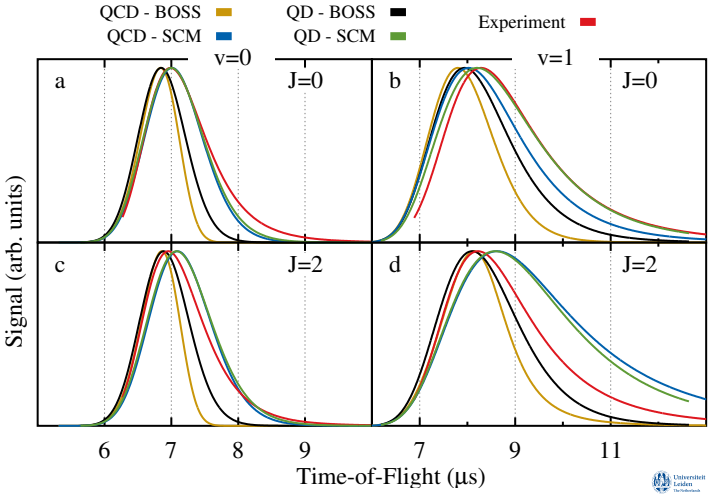

Kaufmann *et al.*, 2018
Smits & Somers, 2023

Rotational and Vibrational Efficacies

- Efficacies (μ) describe the contribution of rot. and vib. energy to the reaction.
  - Fraction of rot/vib energy that can be used to overcome barrier.
  - Depends on geometry of the PES around the barrier.
- Calculated using the treshold offset (ΔS) method.
- Ratio of curve onset change vs rovib. energy change.

$$\mu_{rot}(v, J) = \frac{\Delta S(v, J) - \Delta S(v, 0)}{E_{int}(v, J) - E_{int}(v, 0)} \text{ for } J > 0$$

$$\mu_{vib}(v, J) = \frac{\Delta S(v, 0) - \Delta S(0, 0)}{E_{int}(v, 0) - E_{int}(0, 0)} \text{ for } v > 0$$

Rotational and Vibrational Efficacies

- Efficacies (μ) describe the contribution of rot. and vib. energy to the reaction.
  - Fraction of rot/vib energy that can be used to overcome barrier.
  - Depends on geometry of the PES around the barrier.
- Calculated using the treshold offset (ΔS) method.
- Ratio of curve onset change vs rovib. energy change.

$$\mu_{rot}(v, J) = \frac{\Delta S(v, J) - \Delta S(v, 0)}{E_{int}(v, J) - E_{int}(v, 0)} \text{ for } J > 0$$

$$\mu_{vib}(v, J) = \frac{\Delta S(v, 0) - \Delta S(0, 0)}{E_{int}(v, 0) - E_{int}(0, 0)} \text{ for } v > 0$$

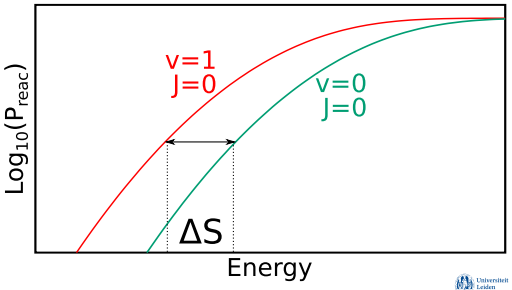

Rotational and Vibrational Efficacies

- Efficacies (μ) describe the contribution of rot. and vib. energy to the reaction.
  - Fraction of rot/vib energy that can be used to overcome barrier.
  - Depends on geometry of the PES around the barrier.
- Calculated using the treshold offset (ΔS) method.
- Ratio of curve onset change vs rovib. energy change.

	QD		QCD		Experiment
	BOSS	SCM	BOSS	SCM	
μ_{vib}	0.593	0.645	0.560	0.595	0.636

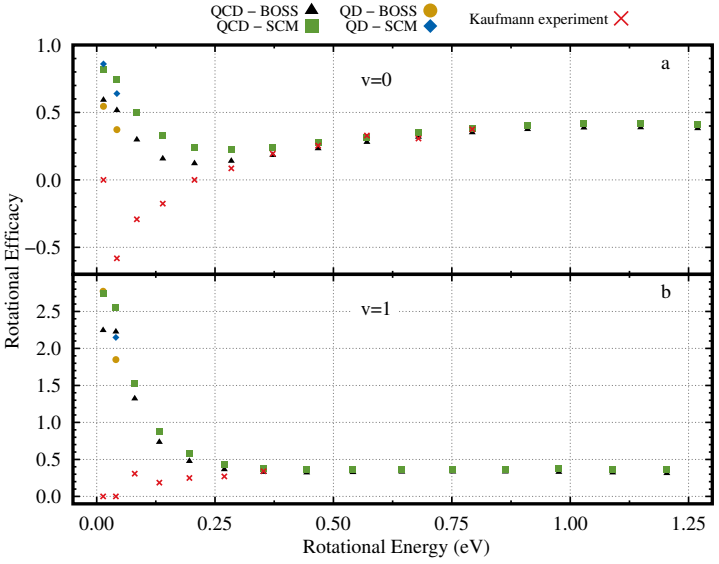

- SCM always predicts slightly higher efficacies.
- Agreement between QD and QCD good.
- No “rotational cooling” in theory results.
- Good agreement with experiment at higher states.

Kaufmann *et al.*, 2018
Smits & Somers, 2023

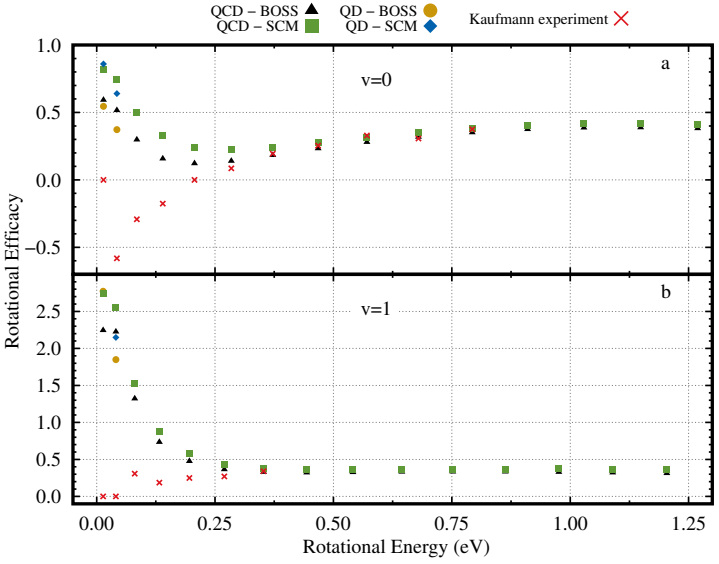

- SCM always predicts slightly higher efficacies.
- Agreement between QD and QCD good.
- No “rotational cooling” in theory results.
- Good agreement with experiment at higher states.

Kaufmann *et al.*, 2018
Smits & Somers, 2023

Rovibrationally elastic scattering

- Imperfections of the PES clear in BOSS results.
  - Averaged out in SCM.
- Vib. ground state clear difference QD↔QCD.
- Vib. excited state better agreement.
  - Higher rovib. energy

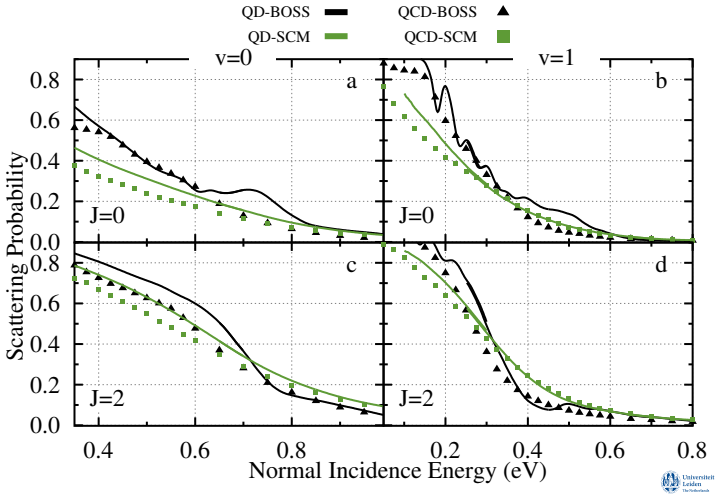

Smits & Somers, 2022

Rovibrationally elastic scattering

- Imperfections of the PES clear in BOSS results.
  - Averaged out in SCM.
- Vib. ground state clear difference QD↔QCD.
- Vib. excited state better agreement.
  - Higher rovib. energy

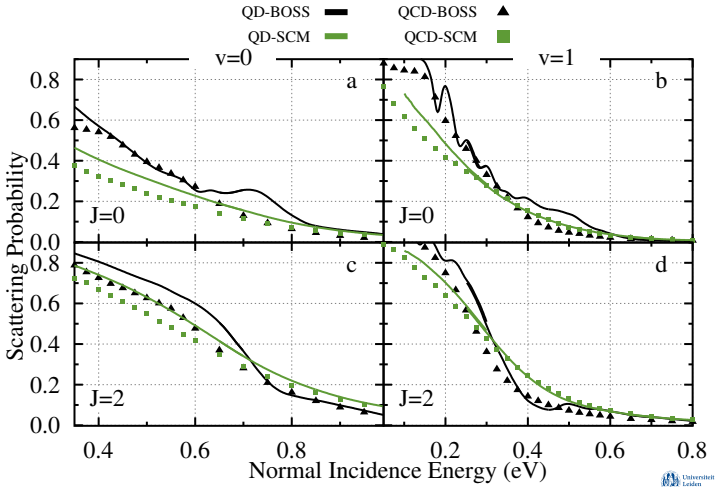

Smits & Somers, 2022

Limited Surface Degrees of Freedom

- Thermal surface effects modeled by displacing a few surface atoms.
  - Past models
  - Computationally cheap(er)
- Cu atom closest to impact site will have the biggest effect.
- Implement SCM, but with slabs of a few atoms.
  - Scale up number of atoms.
  - Get closer to 'real' surface.

Limited Surface Degrees of Freedom

- Thermal surface effects modeled by displacing a few surface atoms.
  - Past models
  - Computationally cheap(er)
- Cu atom closest to impact site will have the biggest effect.
- Implement SCM, but with slabs of a few atoms.
  - Scale up number of atoms.
  - Get closer to 'real' surface.

Elastic scattering on specific surface slabs

One or three distorted surface atoms do not properly describe surface effects.

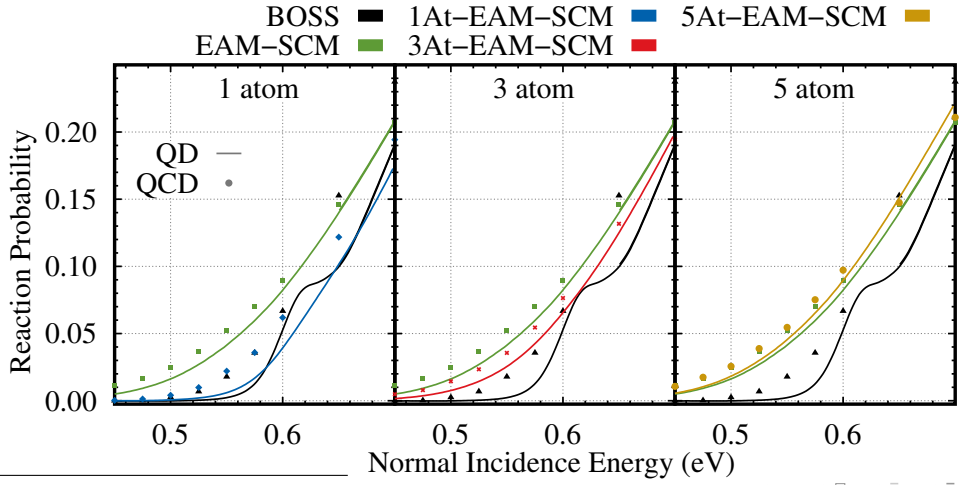

Smits & Somers, 2022

Reduced surface DoF - rovibrationally elastic scattering

Even single distorted surface atom show difference between QD and QCD.

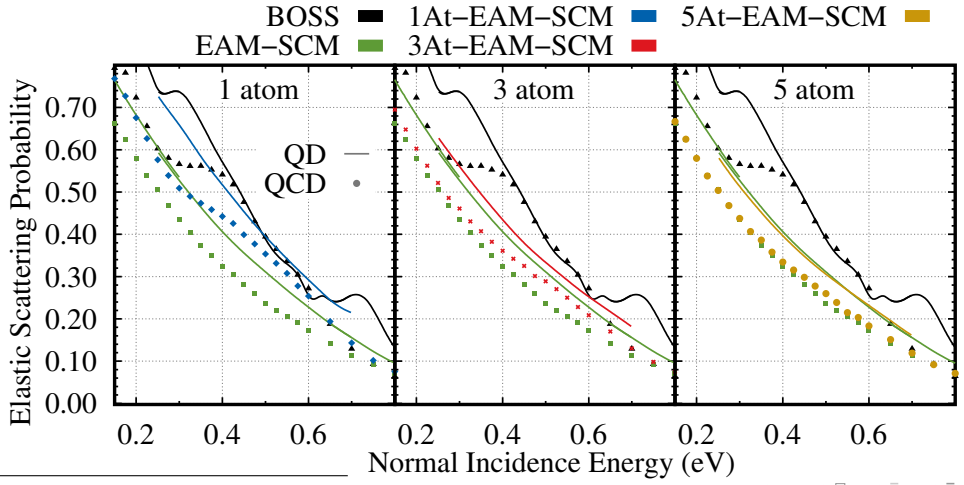

Smits & Somers, 2022

Summary

- SCM improves agreement with experimental results.
- Accurate surface temperature effects for H_2 on Cu(111) at a **quantum dynamical** level with SCM.
  - 104 surface slabs enough for decent convergence of QD-SCM results.
  - QD and QCD reaction agree even for single distorted surface slabs.
- Agreement of simulated time-of-flight spectra demonstrates quality of theory.
  - More direct comparison to experiment.
  - Introduce error due to fitting.
- Theory does not predict “rotational cooling”.
- Need at least 5 surface atoms to describe surface.

Summary

- SCM improves agreement with experimental results.
- Accurate surface temperature effects for H_2 on Cu(111) at a **quantum dynamical** level with SCM.
  - 104 surface slabs enough for decent convergence of QD-SCM results.
  - QD and QCD reaction agree even for single distorted surface slabs.
- Agreement of simulated time-of-flight spectra demonstrates quality of theory.
  - More direct comparison to experiment.
  - Introduce error due to fitting.
- Theory does not predict “rotational cooling”.
- Need at least 5 surface atoms to describe surface.

Summary

- SCM improves agreement with experimental results.
- Accurate surface temperature effects for H_2 on Cu(111) at a **quantum dynamical** level with SCM.
  - 104 surface slabs enough for decent convergence of QD-SCM results.
  - QD and QCD reaction agree even for single distorted surface slabs.
- Agreement of simulated time-of-flight spectra demonstrates quality of theory.
  - More direct comparison to experiment.
  - Introduce error due to fitting.
- Theory does not predict “rotational cooling”.
- Need at least 5 surface atoms to describe surface.

Summary

- SCM improves agreement with experimental results.
- Accurate surface temperature effects for H_2 on Cu(111) at a **quantum dynamical** level with SCM.
  - 104 surface slabs enough for decent convergence of QD-SCM results.
  - QD and QCD reaction agree even for single distorted surface slabs.
- Agreement of simulated time-of-flight spectra demonstrates quality of theory.
  - More direct comparison to experiment.
  - Introduce error due to fitting.
- Theory does not predict “rotational cooling”.
- Need at least 5 surface atoms to describe surface.

Quantum effects for rovibrationally elastic scattering

Acknowledgements

Mark Somers
Geert-Jan Kroes

Mark Wijzenbroek
Paul Spiering

Robert van Bree
Leandra Litjens
Ruard van Workum

Sven Schwabe
Daniel Auerbach
Alec Wodtke

Quantum Dynamics of H_2 on Cu(111) at 925 K: Recent Developments of the Static Corrugation Model

Bauke Smits

Theoretical Chemistry
Leiden University

SDSS 2023
Oktober 7, 2023

Split-Operator Method

$$\Psi(\overrightarrow{Q}; t_0 + \Delta t) =$$
$$\exp\left(-\frac{i}{2}K\Delta t\right)\exp\left(-iV(\overrightarrow{Q})\Delta t\right)$$
$$\exp\left(-\frac{i}{2}K\Delta t\right)\Psi(\overrightarrow{Q}; t_0) + O[(\Delta t)^3]$$

- K Kinetic part of Hamiltonian
- V Potential part of Hamiltonian
- $\overrightarrow{Q}$ 6D position vector of H_2

Random displacements

Original way of generating SCM surface slabs.

- Surface atom displacements are modeled using a random displacement
- Each displacement is sampled from a Gaussian distribution with $\sigma = \sqrt{\frac{3B}{8\pi^2}}$
- B is the Debye-Waller factor for a specific surface temperature
  - Obtained from fits to inelastic neutron scattering
- Displacement assumed to be isotropic and bulk-like

Wijzenbroek & Somers, 2012

Sears & Shelley, 1991

Switched Rydberg function: 2-body and effective 3-body

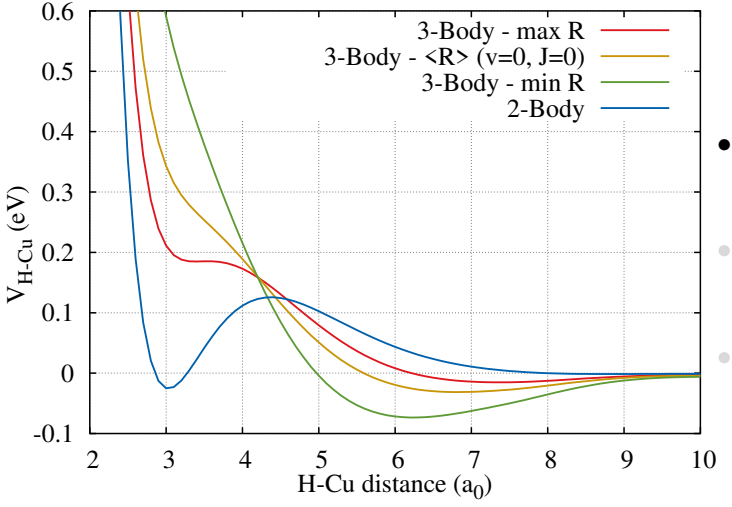

- 3-body and (refitted) 2-body potential.
- 2-body potential only attractive at low H-Cu distances.
- 3-body potential attractive at higher H-Cu distances.

Spiering *et al.*, 2018

Switched Rydberg function: 2-body and effective 3-body

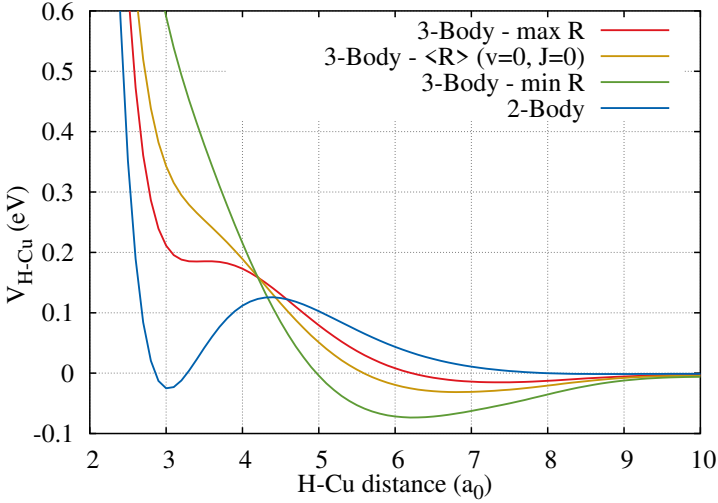

- 3-body and (refitted) 2-body potential.
- 2-body potential only attractive at low H-Cu distances.
- 3-body potential attractive at higher H-Cu distances.

Spiering *et al.*, 2018

SCM thermally distorted surface slabs

1. Originally SCM slabs were generated with random displacement (RD-SCM).
   - Total displacement from Gaussian distribution.
   - Standard deviation from Debye-Waller factor based on T_s.
   - Displacements isotropic and bulk-like.
   - Thermal expansion coefficient from experiment.

2. EAM-SCM uses the embedded atom method (EAM) to generate surface slabs.
   - Displacements from classical dynamics using EAM potential.
   - Potential highly accurate, but unclear fitting pathway.
   - Not based on the same SRP48 functional as the PES and V_{coup}.

Wijzenbroek & Somers, 2012

Sheng *et al.*, 2011

Smits & Somers, 2021

SCM thermally distorted surface slabs

1. Originally SCM slabs were generated with random displacement (RD-SCM).
   - Total displacement from Gaussian distribution.
   - Standard deviation from Debye-Waller factor based on T_s.
   - Displacements isotropic and bulk-like.
   - Thermal expansion coefficient from experiment.

2. EAM-SCM uses the embedded atom method (EAM) to generate surface slabs.
   - Displacements from classical dynamics using EAM potential.
   - Potential highly accurate, but unclear fitting pathway.
   - Not based on the same SRP48 functional as the PES and V_{coup}.

Wijzenbroek & Somers, 2012
Sheng *et al.*, 2011
Smits & Somers, 2021

Embedded Atom Method

- Designed by Daw and Baskes in 1983 based on the quasiatom theory
  - '*A new means of calculating ground-state properties of realistic metal systems*'

1. Each atom is viewed as *embedded* in a host lattice containing all other atoms
2. A pair-wise interaction to model the core-core repulsion

Daw & Baskes, 1983

Embedded Atom Method

- Designed by Daw and Baskes in 1983 based on the quasiatom theory
  - '*A new means of calculating ground-state properties of realistic metal systems*'

1. Each atom is viewed as *embedded* in a host lattice containing all other atoms
2. A pair-wise interaction to model the core-core repulsion

$$E_{\mathrm{EAM}} = \sum_i \left[F(n_i) + \frac{1}{2} \sum_{j \neq i} \phi(r_{ij}) \right]$$

$$n_i = \sum_{j \neq i} \rho(r_{ij})$$

r_{ij} Distance atom i - j
$F(n)$ Embedding function
$\rho(r)$ Density function
$\phi(r)$ Pair function

Daw & Baskes, 1983

Embedded Atom Method

- Designed by Daw and Baskes in 1983 based on the quasiatom theory
  - '*A new means of calculating ground-state properties of realistic metal systems*'

1. Each atom is viewed as *embedded* in a host lattice containing all other atoms
2. A pair-wise interaction to model the core-core repulsion

$$E_{\mathrm{EAM}} = \sum_i \left[F(n_i) + \frac{1}{2} \sum_{j \neq i} \phi(r_{ij}) \right]$$

$$n_i = \sum_{j \neq i} \rho(r_{ij})$$

r_{ij} Distance atom i - j

$F(n)$ Embedding function

$\rho(r)$ Density function

$\phi(r)$ Pair function

Daw & Baskes, 1983

Static Corrugation Model

We construct the full PES from three contributions:

$$V_{DFT}(\vec{q}^{id}, \vec{q}, \vec{r}) = V_{DFT}(\vec{q}^{id}, \vec{r}^{id}(\vec{r})) \quad (1)$$
$$+ V_{coup}(\vec{q}^{id}, \vec{q}, \vec{r}) \quad (2)$$
$$+ V_{strain}(\vec{q}^{id}, \vec{q}) \quad (3)$$

$\vec{q}$ Position surface atoms
$\vec{r}$ Position adsorbates (H_2)

1. Full CRP PES based on DFT with ideal, static surface approximation.

Wijzenbroek & Somers, 2012

Static Corrugation Model

We construct the full PES from three contributions:

$$V_{DFT}(\vec{q}^{\,id}, \vec{q}, \vec{r}) = V_{DFT}(\vec{q}^{\,id}, \vec{r}^{\,id}(\vec{r})) \quad (1)$$
$$+ V_{coup}(\vec{q}^{\,id}, \vec{q}, \vec{r}) \quad (2)$$
$$+ V_{strain}(\vec{q}^{\,id}, \vec{q}) \quad (3)$$

$\vec{q}$ Position surface atoms

$\vec{r}$ Position adsorbates (H_2)

1. Full CRP PES based on DFT with ideal, static surface approximation.
2. $$\sum_i^{\vec{r}} \sum_j^{\vec{q}} \left[V_{H\text{-}Cu}(|\vec{r_i} - \vec{q_j}|) - V_{H\text{-}Cu}(|\vec{r_i}^{\,id}(\vec{r_i}) - \vec{q_j}^{\,id}|) \right]$$

Wijzenbroek & Somers, 2012

Static Corrugation Model

We construct the full PES from three contributions:

$$V_{DFT}(\vec{q}^{\,id}, \vec{q}, \vec{r}) = V_{DFT}(\vec{q}^{\,id}, \vec{r}^{\,id}(\vec{r})) \quad 1$$
$$+ V_{coup}(\vec{q}^{\,id}, \vec{q}, \vec{r}) \quad 2$$
$$+ V_{strain}(\vec{q}^{\,id}, \vec{q}) \quad 3$$

- $\vec{q}$ Position surface atoms
- $\vec{r}$ Position adsorbates (H_2)

1. Full CRP PES based on DFT with ideal, static surface approximation.
2. $$\sum_i^{\vec{r}} \sum_j^{\vec{q}} \left[V_{H\text{-}Cu}(|\vec{r}_i - \vec{q}_j|) - V_{H\text{-}Cu}(|\vec{r}_i^{\,id}(\vec{r}_i) - \vec{q}_j^{\,id}|) \right]$$
3. Surface potential
   - Constant with static surface.

Wijzenbroek & Somers, 2012

Static Corrugation Model

We construct the full PES from two contributions:

$$V_{DFT}(\vec{q}^{\,id}, \vec{q}, \vec{r}) = V_{DFT}(\vec{q}^{\,id}, \vec{r}^{\,id}(\vec{r})) \quad 1$$
$$+ V_{coup}(\vec{q}^{\,id}, \vec{q}, \vec{r}) \quad 2$$
$$+ \cancel{V_{strain}(\vec{q}^{\,id}, \vec{q})} \quad 3$$

- $\vec{q}$ Position surface atoms
- $\vec{r}$ Position adsorbates (H_2)

1. Full CRP PES based on DFT with ideal, static surface approximation.
2. $$\sum_i^{\vec{r}} \sum_j^{\vec{q}} \left[V_{H\text{-}Cu}(|\vec{r}_i - \vec{q}_j|) - V_{H\text{-}Cu}(|\vec{r}_i^{\,id}(\vec{r}_i) - \vec{q}_j^{\,id}|) \right]$$
3. Surface potential
   - Constant with static surface.

Wijzenbroek & Somers, 2012

Static Corrugation Model

We construct the full PES from two contributions:

$$V_{DFT}(\vec{q}^{id}, \vec{q}, \vec{r}) = V_{DFT}(\vec{q}^{id}, \vec{r}^{id}(\vec{r})) \quad (1)$$
$$+ V_{coup}(\vec{q}^{id}, \vec{q}, \vec{r}) \quad (2)$$
$$+ \cancel{V_{strain}(\vec{q}^{id}, \vec{q})} \quad (3)$$

- $\vec{q}$ Position surface atoms
- $\vec{r}$ Position adsorbates (H_2)

1. Full CRP PES based on DFT with ideal, static surface approximation.
2. $$\sum_i^{\vec{r}} \sum_j^{\vec{q}} \left[V_{H\text{-}Cu}(|\vec{r_i} - \vec{q_j}|) - V_{H\text{-}Cu}(|\vec{r_i}^{id}(\vec{r_i}) - \vec{q_j}^{id}|) \right]$$
3. Surface potential
   - Constant with static surface.

Wijzenbroek & Somers, 2012

First version of V_{coup}: 2-body potential

$$\sum_i^{\vec{r}} \sum_j^{\vec{q}} \left[V_{H\text{-}Cu}(|\vec{r_i} - \vec{q_j}|) - V_{H\text{-}Cu}(|\vec{r_i}^{id}(\vec{r_i}) - \vec{q_j}^{id}|) \right]$$

Switched Rydberg function:

$$V_{H\text{-}Cu}(R) = (1 - \rho(R))V(R) + \rho(R)V(P_7)$$

$$V(R) = -e^{-P_4(R-P_5)} \left(\sum_{k=0}^{3} P_k (R - P_5)^k \right)$$

$$\rho(R) = \begin{cases} 0 & \text{for } R < P_6 \\ \frac{1}{2} \cos\left(\frac{\pi(R - P_7)}{P_7 - P_6} \right) + \frac{1}{2} & \text{for } P_6 \leq R \leq P_7 \\ 1 & \text{for } R > P_7 \end{cases}$$

Wijzenbroek & Somers, 2012

First version of V_{coup}: 2-body potential

$$\sum_i^{\vec{r}} \sum_j^{\vec{q}} \left[V_{H\text{-}Cu}(|\vec{r_i} - \vec{q_j}|) - V_{H\text{-}Cu}(|\vec{r_i}^{id}(\vec{r_i}) - \vec{q_j}^{id}|) \right]$$

Switched Rydberg function:

$V_{H\text{-}Cu}(R) = (1 - \rho(R))V(R) + \rho(R)V(P_7)$

$$V(R) = -e^{-P_4(R-P_5)} \left(\sum_{k=0}^{3} P_k (R - P_5)^k \right)$$

$$\rho(R) = \begin{cases} 0 & \text{for } R < P_6 \\ \frac{1}{2} \cos\left(\frac{\pi(R - P_7)}{P_7 - P_6} \right) + \frac{1}{2} & \text{for } P_6 \leq R \leq P_7 \\ 1 & \text{for } R > P_7 \end{cases}$$

Wijzenbroek & Somers, 2012

First version of V_{coup}: 2-body potential

$$\sum_{i}^{\vec{r}} \sum_{j}^{\vec{q}} \left[V_{H\text{-}Cu}(|\vec{r_i} - \vec{q_j}|) - V_{H\text{-}Cu}(|\vec{r_i}^{id}(\vec{r_i}) - \vec{q_j}^{id}|) \right]$$

Switched Rydberg function:

$$V_{H\text{-}Cu}(R) = (1 - \rho(R))V(R) + \rho(R)V(P_7)$$

$$V(R) = -\mathrm{e}^{-\mathrm{P_4}(\mathrm{R}-\mathrm{P_5})} \left(\sum_{\mathrm{k}=0}^{3} \mathrm{P_k}(\mathrm{R} - \mathrm{P_5})^{\mathrm{k}} \right)$$

$$\rho(R) = \begin{cases} 0 & \text{for } R < P_6 \\ \frac{1}{2}\cos\left(\frac{\pi(R - P_7)}{P_7 - P_6}\right) + \frac{1}{2} & \text{for } P_6 \leq R \leq P_7 \\ 1 & \text{for } R > P_7 \end{cases}$$

Wijzenbroek & Somers, 2012

H_2-bond adapted Rydberg function: Effective 3-body

$$P_i = \begin{cases} P_{i,a} R^{min}_{H\text{-}H} + P_{i,b} & \text{for } R_{H\text{-}H} < R^{min}_{H\text{-}H} \\ P_{i,a} R_{H\text{-}H} + P_{i,b} & \text{for } R^{min}_{H\text{-}H} \leq R_{H\text{-}H} \leq R^{max}_{H\text{-}H} \\ P_{i,a} R^{max}_{H\text{-}H} + P_{i,b} & \text{for } R_{H\text{-}H} < R^{max}_{H\text{-}H} \end{cases}$$

- An effective 3-body (H-H-Cu) coupling potential.
  - Designed by Paul Spiering during his master's project.
- A larger set of DFT data allowed for a better fit.
  - 15113 configurations vs 153 configurations.
- Support for different set of parameters for different Cu layers.
  - Only top two layers used for SCM.
  - No sensible results when separate parameters are fitted per layer.

Spiering *et al.*, 2018

H_2-bond adapted Rydberg function: Effective 3-body

$$P_i = \begin{cases} P_{i,a} R^{min}_{H\text{-}H} + P_{i,b} & \text{for } R_{H\text{-}H} < R^{min}_{H\text{-}H} \\ P_{i,a} R_{H\text{-}H} + P_{i,b} & \text{for } R^{min}_{H\text{-}H} \leq R_{H\text{-}H} \leq R^{max}_{H\text{-}H} \\ P_{i,a} R^{max}_{H\text{-}H} + P_{i,b} & \text{for } R_{H\text{-}H} < R^{max}_{H\text{-}H} \end{cases}$$

- An effective 3-body (H-H-Cu) coupling potential.
  - Designed by Paul Spiering during his master's project.
- A larger set of DFT data allowed for a better fit.
  - 15113 configurations vs 153 configurations.
- Support for different set of parameters for different Cu layers.
  - Only top two layers used for SCM.
  - No sensible results when separate parameters are fitted per layer.

Spiering *et al.*, 2018

H_2-bond adapted Rydberg function: Effective 3-body

$$P_i = \begin{cases} P_{i,a} R^{min}_{H\text{-}H} + P_{i,b} & \text{for } R_{H\text{-}H} < R^{min}_{H\text{-}H} \\ P_{i,a} R_{H\text{-}H} + P_{i,b} & \text{for } R^{min}_{H\text{-}H} \leq R_{H\text{-}H} \leq R^{max}_{H\text{-}H} \\ P_{i,a} R^{max}_{H\text{-}H} + P_{i,b} & \text{for } R_{H\text{-}H} < R^{max}_{H\text{-}H} \end{cases}$$

- An effective 3-body (H-H-Cu) coupling potential.
  - Designed by Paul Spiering during his master's project.
- A larger set of DFT data allowed for a better fit.
  - 15113 configurations vs 153 configurations.
- Support for different set of parameters for different Cu layers.
  - Only top two layers used for SCM.
  - No sensible results when separate parameters are fitted per layer.

Spiering *et al.*, 2018

Correction to thermal lattice expansion

$$\sum_i^{\vec{r}} \sum_j^{\vec{d}} \left[V_{H\text{-}Cu}(|\vec{r_i} - \vec{q_j}|) - V_{H\text{-}Cu}(|\vec{r_i}^{id}(\vec{r_i}) - \vec{q_j}^{id}|) \right]$$

Scale the center-of-mass coordinates of the H_2 to their 'ideal lattice' positions.

- Along the lattice vectors.
- Ensures rovib. state is unaffected.

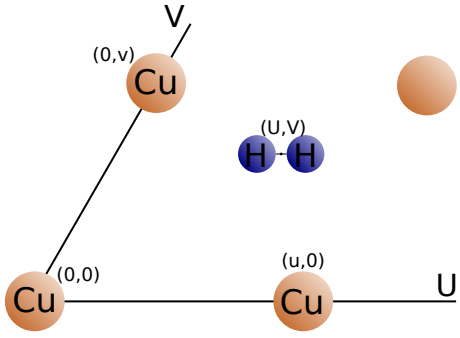

Wijzenbroek & Somers, 2012

Correction to thermal lattice expansion

$$\sum_i^{\vec{r}} \sum_j^{\vec{q}} \left[V_{H\text{-}Cu}(|\vec{r_i} - \vec{q_j}|) - V_{H\text{-}Cu}(|\vec{r_i}^{id}(\vec{r_i}) - \vec{q_j}^{id}|) \right]$$

Scale the center-of-mass coordinates of the H_2 to their 'ideal lattice' positions.

- Along the lattice vectors.
- Ensures rovib. state is unaffected.

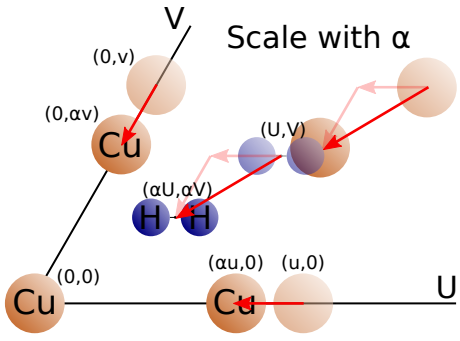

Wijzenbroek & Somers, 2012

Distorted Surface Generation

- Generate surface configurations using molecular dynamics.

- Embedded Atom Method (EAM) potential.
- Database of 25.000 configurations from 1000 MD traces.

Daw & Baskes, 1983
Sheng *et al.*, 2011

Distorted Surface Generation

- Generate surface configurations using molecular dynamics.

- Embedded Atom Method (EAM) potential.
- Database of 25.000 configurations from 1000 MD traces.

$$E_{\mathrm{EAM}} = \sum_i \left[F(n_i) + \frac{1}{2} \sum_{j \neq i} \phi(r_{ij}) \right]$$

$$n_i = \sum_{j \neq i} \rho(r_{ij})$$

r_{ij} Distance atom i - j
$F(n)$ Embedding function
$\rho(r)$ Density function
$\phi(r)$ Pair function

Daw & Baskes, 1983
Sheng *et al.*, 2011

Failure of classical MD

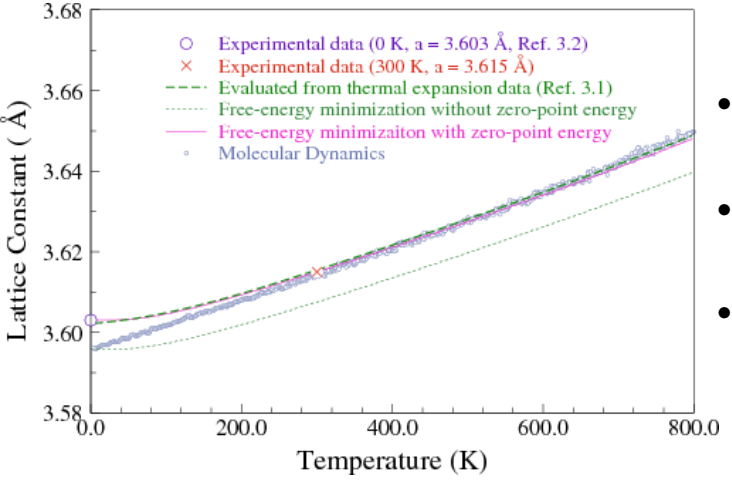

- MD does not always work for surface generation.
- At low T_s, the thermostat extracts zero-point energy.
- Implicit use of Maxwell-Boltzmann distribution for phonons.
  - Actually need Bose-Einstein statistics for bosons.

Sheng *et al.*, 2011

https://sites.google.com/site/eampotentials/Cu

Beyond the static surface

Using the EAM to describe the surface during (classical) dynamics, we can investigate energy exchange.

1. CRP PES describes potential on adsorbate.
2. Use the EAM as the potential for a fully dynamic surface slab.
3. SCM coupling potential describes effect of distorted surface on H_2.
   - Also the full effect of the H_2 on the surface atoms.

- Initialise each surface configuration from EAM generated traces.
  - Position and momentum
- Much more computationally intensive $\rightarrow$ over 200 DoF.

Beyond the static surface

Using the EAM to describe the surface during (classical) dynamics, we can investigate energy exchange.

1. CRP PES describes potential on adsorbate.
2. Use the EAM as the potential for a fully dynamic surface slab.
3. SCM coupling potential describes effect of distorted surface on H_2.
   - Also the full effect of the H_2 on the surface atoms.

- Initialise each surface configuration from EAM generated traces.
  - Position and momentum
- Much more computationally intensive $\rightarrow$ over 200 DoF.

Beyond the static surface

Using the EAM to describe the surface during (classical) dynamics, we can investigate energy exchange.

1. CRP PES describes potential on adsorbate.
2. Use the EAM as the potential for a fully dynamic surface slab.
3. SCM coupling potential describes effect of distorted surface on H_2.
   - Also the full effect of the H_2 on the surface atoms.

- Initialise each surface configuration from EAM generated traces.
  - Position and momentum
- Much more computationally intensive $\rightarrow$ over 200 DoF.

DCM

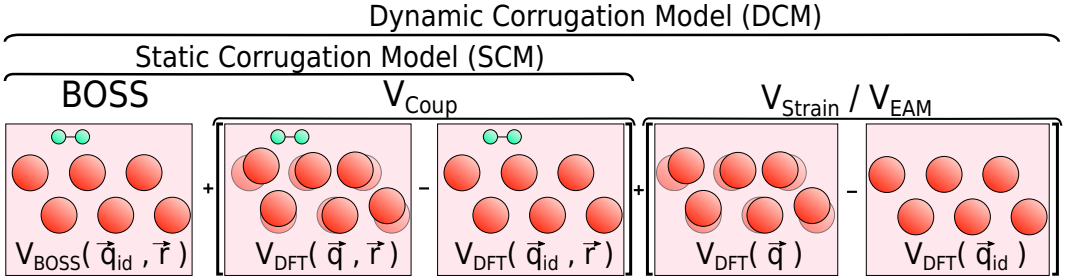
Dynamic Corrugation Model (DCM)
Static Corrugation Model (SCM)
BOSS
V_{Coup}
V_{Strain} / V_{EAM}
+
–
+
–
$V_{BOSS}(\vec{q}_{id}, \vec{r})$
$V_{DFT}(\vec{q}, \vec{r})$
$V_{DFT}(\vec{q}_{id}, \vec{r})$
$V_{DFT}(\vec{q})$
$V_{DFT}(\vec{q}_{id})$

DCM

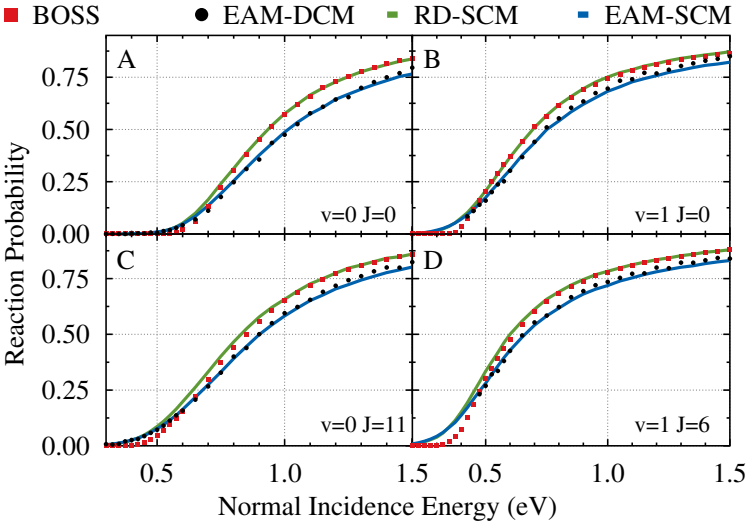
BOSS
EAM-DCM
RD-SCM
EAM-SCM
A
B
C
D
v=0 J=0
v=1 J=0
v=0 J=11
v=1 J=6
Reaction Probability
0.00
0.25
0.50
0.75
0.5
1.0
1.5
Normal Incidence Energy (eV)

	2021 Grid		2022 Grid			
Energy range (eV)	0.25-0.70	0.65-1.00	0.10-0.30	0.25-0.65	0.60-1.05	1.00-1.40
Z_{start} (a_0)	-1.0	-1.0	-1.0	-1.0	-1.0	-1.0
$N_{Z_{spec}}$	256	256	180	180	256	256
N_Z	180	180	128	128	180	240
ΔZ (a_0)	0.15	0.15	0.15	0.15	0.10	0.10
Z_{ana} (a_0)	12.05	12.05	9.20	9.20	9.20	9.20
R_{start} (a_0)	0.60	0.60	0.60	0.60	0.60	0.60
N_r	64	64	64	64	64	64
ΔR	0.15	0.15	0.15	0.15	0.15	0.15
N_x	24	24	24	24	24	24
N_y	24	24	24	24	24	24
Max. J in basis set	18	18	18	18	18	18
Max. m_J in basis set	12	12	12	12	12	12
SCM cutoff (a_0)	16.0	16.0	16.0	16.0	16.0	16.0
Complex absorbing potentials						
Z^{CAP} start (a_0)	12.20	12.20	9.350	9.350	9.300	9.300
Z^{CAP} end (a_0)	25.85	25.85	18.05	18.05	16.90	22.90
Z^{CAP} optimum (eV)	0.125	0.325	0.050	0.125	0.300	0.500
Z^{CAP}_{spec} start (a_0)	31.95	31.95	17.00	17.00	17.40	19.00
Z^{CAP}_{spec} end (a_0)	37.25	37.25	25.85	25.85	24.50	24.50
Z^{CAP}_{spec} optimum (eV)	0.125	0.325	0.050	0.125	0.300	0.500
R^{CAP} start (a_0)	4.200	4.200	4.200	4.200	4.200	4.200
R^{CAP} end (a_0)	10.05	10.05	10.05	10.05	10.05	10.05
R^{CAP} optimum (eV)	0.100	0.100	0.100	0.100	0.100	0.100
Propagation						
Δt ($\hbar/E_h$)	2.5	2.5	1.5	1.5	1.5	1.5
t_f ($\hbar/E_h$)	45000	45000	60000	45000	30000	30000
Initial wave packet						
E_{min} (eV)	0.25	0.65	0.10	0.25	0.60	1.00
E_{max} (eV)	0.70	1.00	0.30	0.65	1.05	1.40
Z_0 (a_0)	21.95	21.95	13.10	13.10	13.30	14.10

mJ dependency? - BOSS

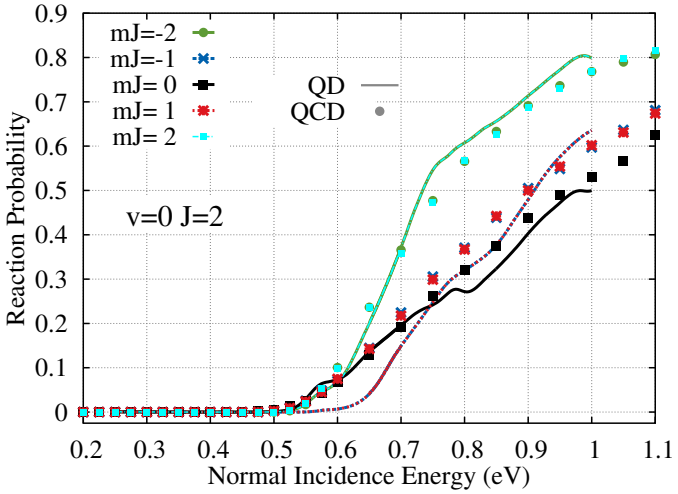

mJ dependency? - EAM-SCM

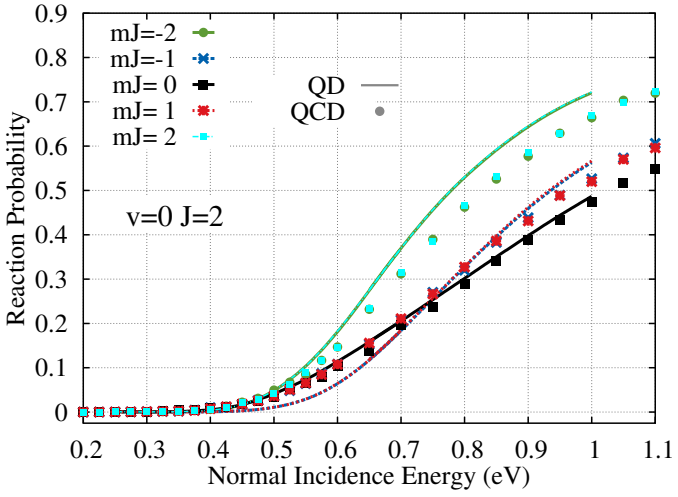

Computational details - Slab generation

1. Equilibrate bulk using NVT (Velocity-Verlet)
   - Berendsen or Langevin thermostat
   - 5 fs stepsize
   - Lattice constant from many bulk relaxations
2. Verify bulk stability in NVE (Bulirsch-Stoer)
3. Equilibrate slab using NVT with static layers
   - No volume rescaling
4. Verify slab stability in NVE
5. Determine 'perfect' lattice positions using NVE
6. Generate surface trace

Computational details - Slab generation

1. Equilibrate bulk using NVT (Velocity-Verlet)
   - Berendsen or Langevin thermostat
   - 5 fs stepsize
   - Lattice constant from many bulk relaxations
2. Verify bulk stability in NVE (Bulirsch-Stoer)
3. Equilibrate slab using NVT with static layers
   - No volume rescaling
4. Verify slab stability in NVE
5. Determine 'perfect' lattice positions using NVE
6. Generate surface trace

Computational details - Slab generation

1. Equilibrate bulk using NVT (Velocity-Verlet)
   - Berendsen or Langevin thermostat
   - 5 fs stepsize
   - Lattice constant from many bulk relaxations
2. Verify bulk stability in NVE (Bulirsch-Stoer)
3. Equilibrate slab using NVT with static layers
   - No volume rescaling
4. Verify slab stability in NVE
5. Determine 'perfect' lattice positions using NVE
6. Generate surface trace

Computational details - Slab generation

1. Equilibrate bulk using NVT (Velocity-Verlet)
   - Berendsen or Langevin thermostat
   - 5 fs stepsize
   - Lattice constant from many bulk relaxations
2. Verify bulk stability in NVE (Bulirsch-Stoer)
3. Equilibrate slab using NVT with static layers
   - No volume rescaling
4. Verify slab stability in NVE
5. Determine 'perfect' lattice positions using NVE
6. Generate surface trace

Computational details - Slab generation

1. Equilibrate bulk using NVT (Velocity-Verlet)
   - Berendsen or Langevin thermostat
   - 5 fs stepsize
   - Lattice constant from many bulk relaxations
2. Verify bulk stability in NVE (Bulirsch-Stoer)
3. Equilibrate slab using NVT with static layers
   - No volume rescaling
4. Verify slab stability in NVE
5. Determine 'perfect' lattice positions using NVE
6. Generate surface trace

Computational details - Slab generation

1. Equilibrate bulk using NVT (Velocity-Verlet)
   - Berendsen or Langevin thermostat
   - 5 fs stepsize
   - Lattice constant from many bulk relaxations
2. Verify bulk stability in NVE (Bulirsch-Stoer)
3. Equilibrate slab using NVT with static layers
   - No volume rescaling
4. Verify slab stability in NVE
5. Determine 'perfect' lattice positions using NVE
6. Generate surface trace

Computational details - Surface slabs

- Copper in bulk and (111) surface
- Supercell of 7x7x7 atoms
- Lowest 3 atom layers static for surfaces
  - In bulk configuration from NVE dynamics
- Periodic boundaries for the x- and y-directions
- Surface configurations from snapshots of NVE dynamics

X and Y

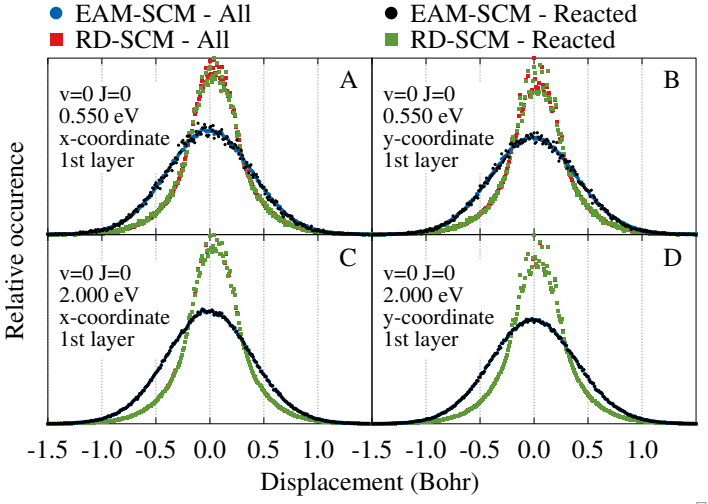
EAM-SCM - All
RD-SCM - All
EAM-SCM - Reacted
RD-SCM - Reacted
A
v=0 J=0
0.550 eV
x-coordinate
1st layer
B
v=0 J=0
0.550 eV
y-coordinate
1st layer
C
v=0 J=0
2.000 eV
x-coordinate
1st layer
D
v=0 J=0
2.000 eV
y-coordinate
1st layer
Relative occurence
-1.5 -1.0 -0.5 0.0 0.5 1.0 -1.5 -1.0 -0.5 0.0 0.5 1.0
Displacement (Bohr)

Z

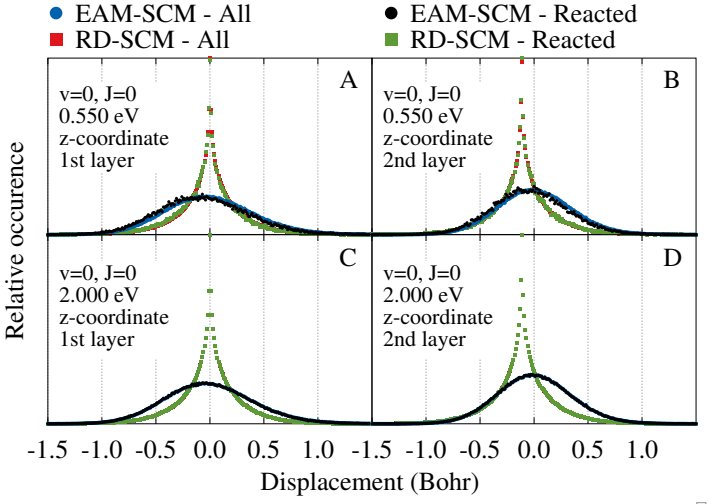
EAM-SCM - All
RD-SCM - All
EAM-SCM - Reacted
RD-SCM - Reacted
A
v=0, J=0
0.550 eV
z-coordinate
1st layer
B
v=0, J=0
0.550 eV
z-coordinate
2nd layer
C
v=0, J=0
2.000 eV
z-coordinate
1st layer
D
v=0, J=0
2.000 eV
z-coordinate
2nd layer
Relative occurence
-1.5 -1.0 -0.5 0.0 0.5 1.0 -1.5 -1.0 -0.5 0.0 0.5 1.0
Displacement (Bohr)

Time-of-Flight spectra

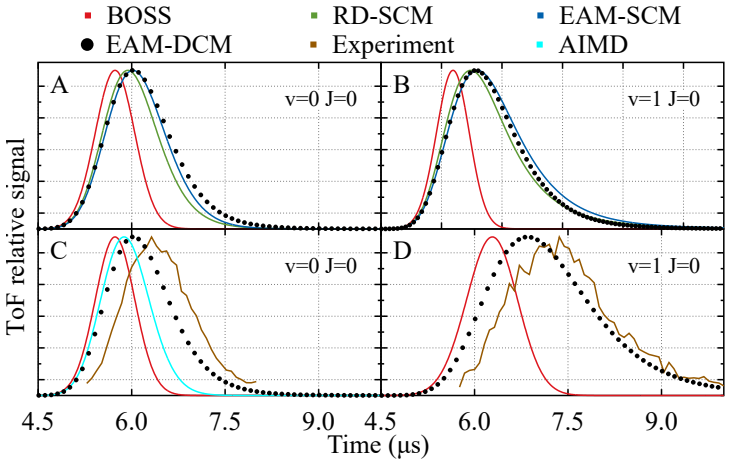

Smits & Somers, 2021

- Good agreement between SCM and DCM.

Time-of-Flight spectra

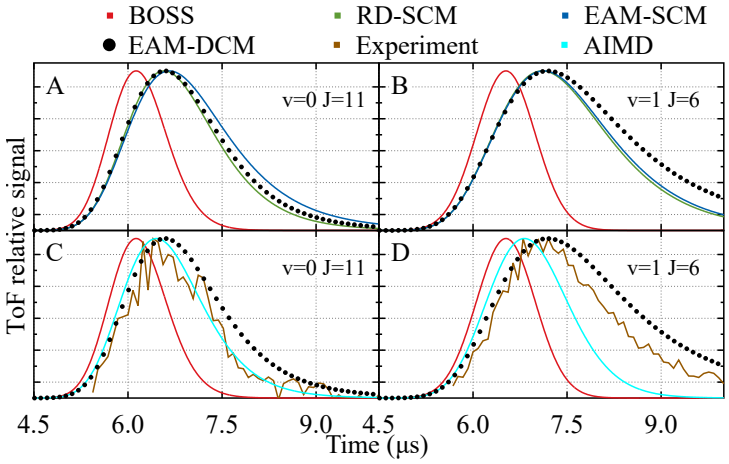

Smits & Somers, 2021

- Agreement with experiment about equal to AIMD.

Some binning methods

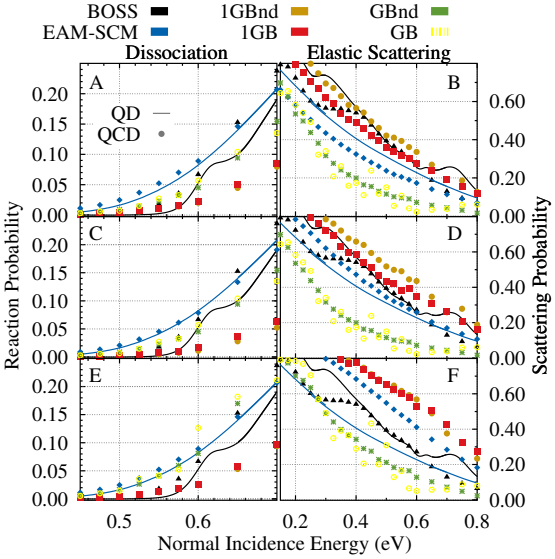

- Some minor improvement when using different binning techniques.
- No adiabatic correction! (yet??)